Critical Amino Acid Residues Determine the Binding Affinity and the Ca $^{2+}$ Release Efficacy of Maurocalcine in Skeletal Muscle Cells

Eric Estève, Sophia Smida-Rezgui, Sandor Sarkozi, Csaba Szegedi, Imed Regaya, Lili Chen, Xavier Altafaj, Hervé Rochat, Paul Allen, Isaac N. Pessah, Isabelle Marty, Jean-Marc Sabatier, Istvan Jona, Michel De Waard and Michel Ronjat

Access the most updated version of this article at doi: 10.1074/jbc.M305798200

Find articles, minireviews, Reflections and Classics on similar topics on the JBC Affinity Sites.

Alerts:

- When this article is cited
- When a correction for this article is posted

Click here to choose from all of JBC's e-mail alerts

This article cites 22 references, 8 of which can be accessed free at
http://www.jbc.org/content/278/39/37822.full.html#ref-list-1

Critical Amino Acid Residues Determine the Binding Affinity and the Ca²⁺ Release Efficacy of Maurocalcine in Skeletal Muscle Cells*

Eric Estève‡§¶, Sophia Smida-Rezgui‡∥, Sandor Sarkozi, Csaba Szegedi**, Imed Regaya§,
Lili Chen‡‡, Xavier Altafaj‡, Hervé Rochat§, Paul Allen§§, Isaac N. Pessah‡‡¶¶, Isabelle Marty‡,
Jean-Marc Sabatier§, Istvan Jona**, Michel De Waard‡, and Michel Ronjat‡∥∥∥**

*From the ‡INSERM EMI 9931, CEA, CIS, 17 Rue des Martyrs, 38054 Grenoble Cedex 09, France, **Department of
Physiology, University Medical School of Debrecen, H-4012, Debrecen, Hungary, §CNRS UMR 6560, Faculté de Médecine
Nord, Boulevard Pierre Dramard, 13916 Marseille Cedex 20, France, ‡‡Department of Molecular Biosciences and
Graduate Program in Neurosciences, University of California, Davis, California 95616, and §§Department of Anesthesia,
Brigham and Women's Hospital, Boston, Massachusetts 02115*

   Maurocalcine (MCa) is a 33 amino acid residue peptide toxin isolated from the scorpion *Scorpio maurus palmatus*. MCa and mutated analogues were chemically synthesized, and their interaction with the skeletal muscle ryanodine receptor (RyR1) was studied on purified RyR1, sarcoplasmic reticulum (SR) vesicles, and cultured myotubes. MCa strongly potentiates [³H]ryanodine binding on SR vesicles (7-fold at pCa 5) with an apparent EC_{50} of 12 nM. MCa decreases the sensitivity of [³H]ryanodine binding to inhibitory high Ca²⁺ concentrations and increases it to the stimulatory low Ca²⁺ concentrations. In the presence of MCa, purified RyR1 channels show long-lasting openings characterized by a conductance equivalent to 60% of the full conductance. This effect correlates with a global increase in Ca²⁺ efflux as demonstrated by MCa effects on Ca²⁺ release from SR vesicles. In addition, we show for the first time that external application of MCa to cultured myotubes produces a cytosolic Ca²⁺ increase due to Ca²⁺ release from 4-chloro-*m*-cresol-sensitive intracellular stores. Using various MCa mutants, we identified a critical role of Arg²⁴ for MCa binding onto RyR1. All of the other MCa mutants are still able to modify [³H]ryanodine binding although with a decreased EC_{50} and a lower stimulation efficacy. All of the active mutants produce both the appearance of a subconductance state and Ca²⁺ release from SR vesicles. Overall, these data identify some amino acid residues of MCa that support the effect of this toxin on ryanodine binding, RyR1 biophysical properties, and Ca²⁺ release from SR.

   In skeletal muscles, contraction is triggered by the massive release of Ca²⁺ from sarcoplasmic reticulum (SR).[1] The channel responsible for this release is the type-1 ryanodine receptor (RyR1). RyR1 has been intensively studied because of its unique structural and functional organization. It forms part of a calcium mobilization complex in which RyR1 is apposed to the L-type voltage-dependent calcium channel (dihydropyridine receptor, DHPR) along many other structural and regulatory components (1). The activation of RyR1 requires a chain of events that starts with plasma membrane depolarization inducing a change in the conformation of DHPR itself transmitted to RyR1. The entire set of events is called excitation-contraction coupling (EC coupling).

   In vitro, the activity of RyR1 can be modulated by a number of different effectors such as Ca²⁺, ryanodine, ATP, caffeine, and 4-chloro-*m*-cresol (CMC) (2, 3). Among these effectors, only few present high selectivity and affinity for RyR1. More specific pharmacological agents for RyR1 have been discovered in scorpion venoms (4, 5). One such peptide has been isolated from the venom of the chactid scorpion *Scorpio maurus* palmatus and has been termed maurocalcine (MCa). It is a 33-mer basic peptide reticulated by three disulfide bridges. MCa can be chemically synthesized without any loss of activity (5). It is potently active on RyR1 as it alters channel properties in the low nanomolar range (5, 6). MCa presents a strong sequence homology (82% amino acid sequence identity) with imperatoxin A (IpTxA), a toxin active on RyR1 and isolated from another scorpion venom (7–10). Besides the fact that MCa and IpTxA represent two of the most high affinity effectors of RyR1, they also share some amino acid sequence homology with a specific domain (domain A) of the II–III loop of $Ca_v\alpha_{1.1}$, the subunit that carries the voltage sensor of DHPR (Fig. 1). Although the exact role of the domain A in the EC-coupling process is highly debated (11–13), we have recently shown by using plasmon resonance measurements that it is the single II–III loop sequence interacting with RyR1 (14). Nevertheless, this exceptional form of homology between a channel sequence and a toxin could be indicative that domain A possesses some kind of yet unresolved function in RyR1 regulation. Therefore, studying the MCa effects on RyR1 may produce several interesting hints on how to proceed further on investigating the role of domain A in EC coupling.

   In this work, we synthesized several MCa analogues in which amino acid residues, also present in homologous position in domain A, were substituted by alanine residues. We then analyzed the effect of MCa and the analogues on [³H]ryanodine

   [1] The abbreviations used are: SR, sarcoplasmic reticulum; RyR1, ryanodine receptor; DHPR, dihydropyridine receptor; IpTxA, imperatoxin A; Fmoc, *N*-(9-fluorenyl)methoxycarbonyl; MOPS, 3-(*N*-morpholino)propanesulfonic acid; PIPES, 1,4-piperazinediethanesulfonic acid;

LLSS, long-lasting subconductance state; EC, excitation-contraction; CMC, 4-chloro-*m*-cresol; MCa, maurocalcine.

This paper is available on line at http://www.jbc.org

binding, Ca^{2+}-dependent activation of RyR1, channel activity, and Ca^{2+} release from SR vesicles. We identified an amino acid residue critical for the interaction of MCa with RyR1 and for the induction of a long-lasting subconductance state. The data also demonstrate a clear relationship in the ability of MCa to potentiate [^{3}H]ryanodine binding, induce a subconductance state, and produce Ca^{2+} release from heavy SR vesicles. To prove the physiological relevance of RyR1 as the main target of MCa, we tested the effect of the peptide on internal Ca^{2+} release in intact myotubes. We show that the addition of 100 nM MCa in Ca^{2+}-free extracellular medium induces an increase in cytosolic Ca^{2+} concentration and a complete inhibition of CMC-induced Ca^{2+} release.

EXPERIMENTAL PROCEDURES

Chemical Synthesis—N-α-Fmoc-L-amino acids, 4-hydroxymethylphenyloxy resin, and reagents used for peptide synthesis were obtained from PerkinElmer Life Sciences. The MCa and analogues were obtained by the solid-phase peptide synthesis (15) using an automated peptide synthesizer (Model 433A, Applied Biosystems Inc.). Analogues were obtained by point mutation (Ala instead of one amino acid in the sequence of maurocalcine native-like) and named Ala/Lys[8], Ala/Lys[19], Ala/Lys[20], Ala/Lys[22], Ala/Arg[23], Ala/Arg[24], and Ala/Thr[26]. Peptide chains were assembled stepwise on 0.25 meq of hydroxymethylphenyloxy resin (1% cross-linked; 0.89 meq of amino group/g) using 1 mmol of N-α-Fmoc amino acid derivatives. The side chain-protecting groups were as follows: trityl for Cys and Asn; *tert*-butyl for Ser, Thr, Glu, and Asp; pentamethylchroman for Arg; and *tert*-butyloxycarbonyl for Lys. N-α-Amino groups were deprotected by treatment with 18 and 20% (v/v) piperidine/N-methylpyrrolidone for 3 and 8 min, respectively. The Fmoc-amino acid derivatives were coupled (20 min) as their hydroxybenzotriazole active esters in N-methylpyrrolidone (4-fold excess). After peptide chain assembly, the peptide resin (approximately 1.8 μg) was treated between 2 and 3 h at room temperature in constant shaking with a mixture of trifluoroacetic acid/H_2O/thioanisol/ethanedithiol (88:5/5/2, v/v) in the presence of crystalline phenol (2.25 g). The peptide mixture was then filtered, and the filtrate was precipitated by adding cold *t*-butylmethyl ether. The crude peptide was pelleted by centrifugation (3.000 $\times$ *g* for 10 min), and the supernatant was discarded. The reduced peptide was then dissolved in 200 mM Tris-HCl buffer, pH 8.3, at a final concentration of 2.5 mM and stirred under air to allow oxidation/folding (between 50 and 72 h, room temperature). The target products, MCa and analogues, were purified to homogeneity, first by reversed-phase high pressure liquid chromatography (PerkinElmer Life Sciences, C_{18} Aquapore ODS, 20 μm, 250 $\times$ 10 mm) by means of a 60-min linear gradient of 0.08% (v/v) trifluoroacetic acid = 0–30% acetonitrile in 0.1% (v/v) trifluoroacetic acid/H_2O at a flow rate of 6 ml/min (λ = 230 nm). A second step of purification of MCa and analogues was achieved by ion-exchange chromatography on a carboxymethyl cellulose matrix using 10 mM (buffer A) and 500 mM (buffer B) sodium phosphate buffers, pH 9.0 (60-min linear gradient from 0 to 60% buffer B at a flow rate of 1 ml/min). The homogeneity and identity of MCa or analogues were assessed by the following: (i) analytical C_{18} reversed-phase high pressure liquid chromatography (Merck, C_{18} LiChrospher, 5 μm, 4 $\times$ 200 mm) using a 60-min linear gradient of 0.08% (v/v) trifluoroacetic acid/0–60% acetonitrile in 0.1% (v/v) trifluoroacetic acid/H_2O at a flow rate of 1 ml/min; (ii) amino acid analysis after acidolysis (6 N HCl/2% (w/v) phenol, 20 h, 118 °C, N_2 atmosphere); and (iii) mass determination by matrix-assisted laser desorption ionization time-of-flight mass spectrometry.

Heavy SR Vesicles Preparation—Heavy SR vesicles were prepared following a modified method of Kim *et al.* (16) as described in Marty *et al.* (17). Protein concentration was measured by the Biuret method.

[^{3}H]Ryanodine Binding Assay—Heavy SR vesicles (1 mg/ml) were incubated at 37 °C for 2.5 h in an assay buffer composed of 5 nM [^{3}H]ryanodine (unless otherwise stated), 150 mM NaCl, 2 mM EGTA, variable concentrations of $CaCl_2$ to adjust for *p*Ca, and 20 mM HEPES, pH 7.4. MCa or peptide mutants were added to the assay buffer just prior to the addition of heavy SR vesicles. [^{3}H]Ryanodine bound to heavy SR vesicles was measured by filtration through Whatmann GF/B glass filters followed by three washes with 5 ml of ice-cold washing buffer composed of 150 mM NaCl, 20 mM HEPES, pH 7.4. Filters were then soaked overnight in 10 ml of scintillation mixture (Cybscint, ICN), and bound radioactivity was determined by scintillation spectrometry. Nonspecific binding was measured in the presence of 20 μM cold ryanodine. Each experiment was performed in triplicate and repeated at

least twice. All of the data are presented as the mean $\pm$ S.E.

Ca^{2+} Release Measurements—Ca^{2+} release from heavy SR vesicles was measured using the Ca^{2+}-sensitive dye, antipyrylazo III. The absorbance was monitored at 710 nm by a diode array spectrophotometer (MOS-200 Optical System, Biologic, Claix, France). Heavy SR vesicles (50 μg) were actively loaded with Ca^{2+} at 37 °C in a 2-ml buffer containing 100 mM KCl, 7.5 mM sodium pyrophosphate, 20 mM potassium MOPS, pH 7.0, supplemented with 250 μM antipyrylazo III, 1 mM ATP/$MgCl_2$, 5 mM phosphocreatine, and 12 μg/ml creatine phosphokinase (18). Ca^{2+} loading was started by sequential additions of 50 and 20 μM of $CaCl_2$. In these loading conditions, no calcium-induced calcium release interferes with the observations. At the end of each experiment, Ca^{2+} remaining in the vesicles was determined by the addition of Ca^{2+} ionophore A23187 (4 μM) and the absorbance signal calibrated by two consecutive additions of 20 μM $CaCl_2$.

RyR1 Ca^{2+} Channel Reconstitution and Single-channel Recording Analysis—Measurements of channel activity were carried out using purified RyR1 incorporated into planar lipid bilayers. RyR1 was purified from rabbit SR vesicles as previously described (19). The bilayers were formed using phosphatidylethanolamine, phosphatidylserine, and L-phosphatidylcholine in a ratio of 5:4:1 dissolved in *n*-decane up to the final lipid concentration of 20 mg/ml (20). Bilayers were formed across a 200- or 250-μm diameter aperture of a Delrin cap using a symmetrical buffer solution (250 mM KCl, 100 μM EGTA, 150 μM $CaCl_2$, 20 mM PIPES, pH 7.2). The chamber into the small aliquot of purified RyR1 was added and defined as the *cis* (cytoplasmic) side, whereas the other chamber labeled as the *trans* (luminal) side was kept on ground potential. To ensure the orientation of the incorporated RyR1, we tested the effect of free Ca^{2+} concentration on both side. After successful incorporation of the RyR1 channel, free calcium concentration in the *cis* chamber was adjusted to 238 nM by the addition of EGTA. Electrical signals were filtered at 1 kHz through an 8-pol low-pass Bessel filter and digitized at 3 kHz using Axopatch 200 and pCLAMP 6.03 (Axon Instruments, Union City, CA).

Total recording time in each experiment was 10–20 min for any experimental condition tested. After changing conditions, at least 5 min were allowed for equilibration, which appeared to be enough to reach the new equilibrium of the parameters. Single channel measurements were carried out at 20–22 °C. The free Ca^{2+} concentration was calculated using the computer program and affinity constants published by Fabiato (21). Open probabilities were calculated using the common 50% criteria with a medial dead zone of 5%. Current amplitude distribution was analyzed using Origin (Microcal Software, Northampton, MA). Values of the open probability are expressed as the means $\pm$ S.E.

Cell Culture—Primary cultures of rat skeletal muscle satellite cells were obtained as described previously (16). Cells were seeded on laminin-coated plates, in a proliferation medium composed of Ham's F-10 with glutamax-I (Invitrogen) supplemented with 20% fetal calf serum (Invitrogen), 2.5 ng/ml basic fibroblast growth factor (Invitrogen), and 1% penicillin-streptomycin (Invitrogen) at 37 °C and 5% CO_2. After 2–3 days, differentiation of satellite cells into myotubes was induced with Dulbecco's modified Eagle's medium with glutamax-I (Invitrogen) supplemented with 10% horse serum (Invitrogen).

Ca^{2+} Imaging from Culture Myotubes—Changes in cytosolic calcium levels were monitored using the calcium-dependent fluorescent dye Fluo-4 (Molecular Probes). The myotubes were loaded for 1 h at room temperature in the presence of 5 μM Fluo-4-AM. Uptake of the dye was facilitated by the addition of 0.02% pluronic acid (Sigma). After loading, myotubes were washed for 1 h to allow ester hydrolysis of the dye. Fluorescence changes were measured by confocal laser-scanning microscopy using a LEICA TCS-SP2 operating system in the xyt mode. Fluo4 was excited at a wavelength of 488 nm, and the fluorescence was collected from 500 to 570 nm. Images were collected every 1.6 s for 2–4 min and then analyzed frame by frame with the data analysis software provided by Leica. Fluorescence curves are expressed as a function of time as $\Delta F/F$, where *F* represents the base-line fluorescence and ΔF represents the fluorescence variations.

RESULTS

Synthesis of MCa and Analogues—Fig. 1 presents the primary structure of the different MCa analogues that we synthesized. The structural determination of MCa shows that the stretch of basic residues (from Lys[20] to Arg[24]) forms a single basic-rich surface (22). We will define the residues forming this basic surface as residues belonging to the "basic class." The opposite surface of the toxin contains four acidic residues (Asp[2],
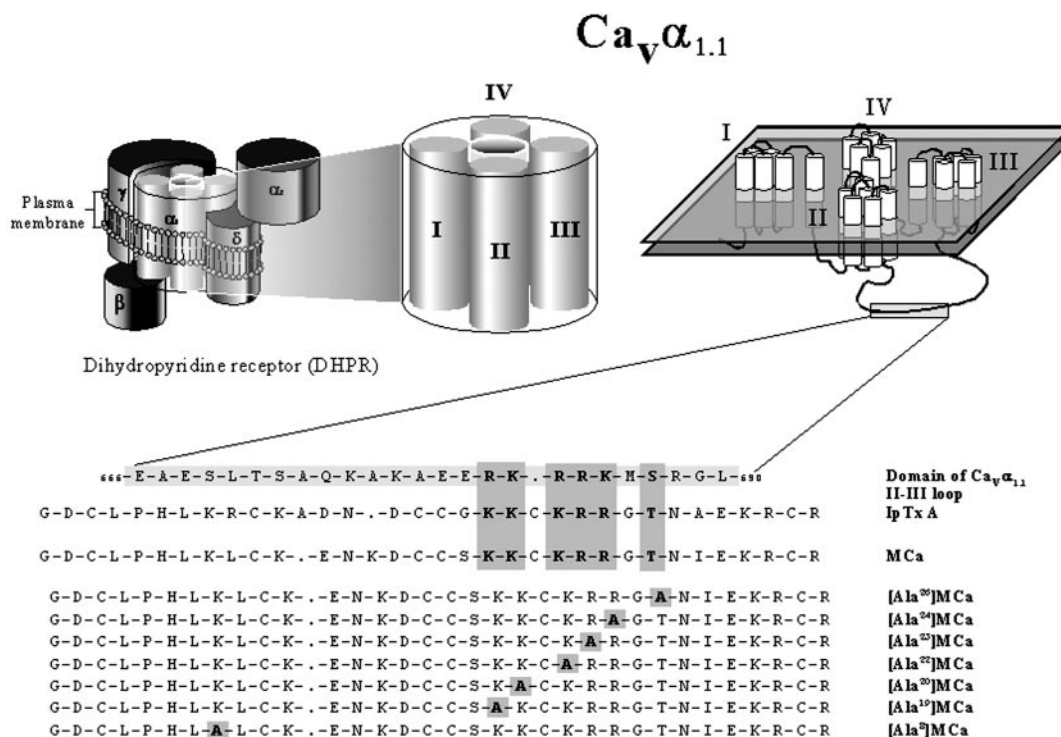
FIG. 1. **Sequence alignment of domain A, IpTxA, MCa, and MCa analogues.** Schematic representation of the DHPR complex illustrating the subunit composition. MCa has sequence similarities with domain A of the II–III loop from the $Ca_v\alpha_{1.1}$ subunit of DHPR and with IpTxA, another scorpion toxin. The homology stretches from Lys[19] to Thr[26] of MCa. The primary structure of the mutated MCa analogues is also shown.

Glu[12], Asp[15], and Glu[29]) and one basic residue (Lys[8]). We will define this acidic surface as the "acidic face." This electrostatic charge distribution creates a marked anisotropy in which the role in MCa pharmacology is unknown. We choose to substitute one by one all of the MCa amino acid residues common between MCa and the domain A of the II–III loop of $Ca_v\alpha_{1.1}$ subunit. Most of these residues belong to the basic class with the exception of Thr[26] and therefore were replaced by neutral alanine residues. We also synthesized the mutant [Ala[8]]MCa because Lys[8] is not conserved in the II–III loop but is located on the toxin face opposite to the basic surface (23). All of the peptides were folded/oxidized in a 200 mM Tris-HCl buffer, pH 8.3, by a 72-h exposure to air and purified to homogeneity by preparative C_{18} reversed-phase high pressure liquid chromatography. Both analysis of elution profiles and circular dichroism spectra indicate that all of the peptides have proper secondary structures (data not shown).

Effects of MCa on [³H]Ryanodine Binding to RyR1—We recently described that MCa stimulates the binding of [³H]ryanodine onto heavy SR vesicles that contain RyR1 (6). Fig. 2A confirms this initial finding as we observe that 200 nM MCa increases the binding of [³H]ryanodine by 7.4 ± 2.5-fold with an EC_{50} of 12.5 ± 0.8 nM. Results presented in Fig. 2B show that MCa induces a slight change in the [³H]ryanodine binding k_{obs} value ($k_{obs} = 1.08 \times 10^{-2} \pm 0.22 \times 10^{-2}$ min^{-1} without MCa *versus* $k_{obs} = 1.81 \times 10^{-2} \pm 0.23 \times 10^{-2}$ min^{-1} with 100 nM MCa). As shown in Fig. 2C, [³H]ryanodine binding on RyR highlights both a high affinity (51 nM) and a low affinity (228 nM) class of binding sites, whereas in the presence of MCa (100 nM), ryanodine binding on RyR1 exhibits a single class of high affinity binding site (11 nM). These results suggest that the increase of ryanodine binding induced by MCa may be because of a conversion of both classes of binding sites into a higher affinity class of binding site. Because [³H]ryanodine binding on SR vesicles is sensitive to external Ca^{2+} concentration, we examined the effect of MCa on [³H]ryanodine binding in the

presence of varying external Ca^{2+} concentrations (Fig. 2D). In the presence of MCa (saturating 100 nM), [³H]ryanodine binding on SR vesicles still shows a classical bell-shaped dependence to external Ca^{2+}. Interestingly, we observed that the [³H]ryanodine binding inhibition by high Ca^{2+} concentration (*p*Ca 3) was slightly decreased, whereas the [³H]ryanodine binding stimulation by low Ca^{2+} concentration (*p*Ca 6 and 6.5) was increased. Indeed, while in the absence of MCa, ryanodine binding was almost completely inhibited (>99%) at pCa 3. In the presence of MCa, 39% of the maximum [³H]ryanodine binding was still observed at *p*Ca 3. Similarly, at *p*Ca 6.5, ryanodine binding is at 70% of its maximum in the presence of MCa, whereas it is only at 4.8% of its maximum in the absence of MCa.

Characterization of the Effects of MCa Mutants on [³H]Ryanodine Binding to RyR1—All of the MCa analogues also stimulate [³H]ryanodine binding (Fig. 3A) with the exception of [Ala[24]]MCa (up to 5 μM). For all of the functional analogues, the EC_{50} of the stimulatory effect is reduced with values ranging between 49 ± 14 nM for [Ala[26]]MCa and 432 ± 168 nM for [Ala[22]]MCa, which would correspond to a reduction of affinity between 4- and 35-fold. [Ala[8]]MCa also appeared less effective than MCa with an EC_{50} of 199 ± 19 nM. These data show that the amino acid residues of MCa can be classified in three different groups: (i) residues belonging to the basic class that are important for interaction with RyR1 (Lys[22], Arg[23], and Arg[24]); (ii) residues belonging or not to the basic class that appear less important for the interaction with RyR1 (Lys[19], Lys[20], and Thr[26]); and (iii) a residue of the acidic face that appears to mildly affect the interaction with RyR1 (Lys[8]). Besides various effects on EC_{50}, all of the active analogues also present a significant decrease on the stimulation efficacy on [³H]ryanodine binding. The stimulation efficacies of the analogues are on average 1.9-fold less than MCa itself and ranged between 3.2 ± 0.4-fold for [Ala[23]]MCa and 4.7 ± 0.1-fold for [Ala[8]]MCa. [Ala[23]]MCa combines two negative changes com-
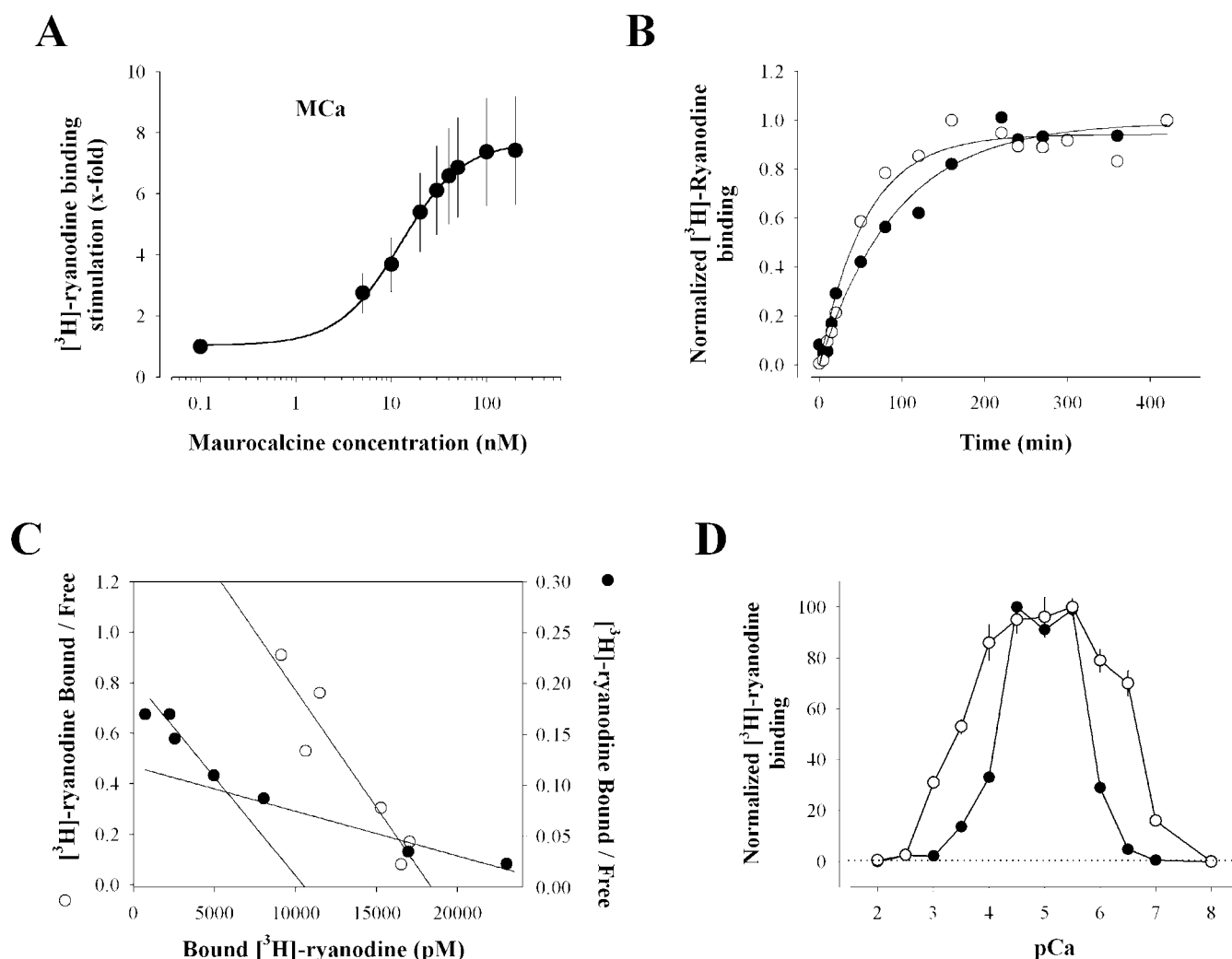
FIG. 2. **MCa affects [³H]ryanodine binding on heavy SR vesicles.** *A*, MCa concentration dependence of [³H]ryanodine binding stimulation. [³H]Ryanodine binding was measured at *p*Ca 5 in the presence of 5 nM [³H]ryanodine for 2.5 h at 37 °C. Nonspecific binding remained constant at all of the MCa concentrations and represented <8% of total binding. Data were fitted with a sigmoid function $y = y_o + (a \times x^b/c^b + x^b)$, where $y_o = 1.0 \pm 0.1$ at MCa = 0 nM, $a = 6.7 \pm 0.2$ is the maximum stimulation factor over basal value, $b = 1.3 \pm 0.1$ the slope coefficient, and $c = 12.5 \pm 0.8$ nM is the EC_{50} for MCa effect. *B*, kinetics of [³H]ryanodine binding in the absence (*filled circles*) and presence of 100 nM MCa (*open circles*). Data were fitted with an exponential curve $y = a \times (1 - \exp(-k_t))$ with a being the maximal achievable normalized binding and k being the pseudo first order rate constant (k_{obs}) value for [³H]ryanodine binding. $a = 0.99 \pm 0.01$ and $k_{obs} = 1.08 \times 10^{-2} \pm 0.22 \times 10^{-2}$ min^{-1} (without MCa), and $a = 0.94 \pm 0.01$ and $k_{obs} = 1.81 \times 10^{-2} \pm 0.23 \times 10^{-2}$ min^{-1} (with 100 nM MCa). *C*, Scatchard representation of the concentration-dependent [³H]ryanodine binding in the absence (*filled circles*) and presence of 100 nM MCa (*open circles*). Experimental conditions in *B* and *C* were as described in *A*. *D*, extravesicular Ca²⁺ concentration dependence of [³H]ryanodine binding in the absence (*filled circles*) and presence of 100 nM MCa (*open circles*). The experiments were performed with 5 nM [³H]ryanodine for 2.5 h at 37 °C.

pared with wild-type MCa, a decrease in the apparent affinity and the lowest [³H]ryanodine binding stimulation efficacy. Two explanations can be put forward to explain why [Ala²⁴]MCa is ineffective on [³H]ryanodine binding. Firstly, it may not bind to RyR1, which is the simplest hypothesis. Secondly, it may bind onto RyR1 but cannot produce allosteric changes required to enhance [³H]ryanodine binding. In this latest case, [Ala²⁴]MCa would compete with MCa for binding on RyR1. To test this hypothesis, we measured the effect of MCa (20 and 100 nM) on [³H]ryanodine binding in the presence of increasing concentrations of [Ala²⁴]MCa. Fig. 3*B* shows that the effect of MCa is not altered by the presence of up to 1 μM [Ala²⁴]MCa, demonstrating that this analogue is not able to bind onto RyR1. We also checked whether or not the absence of the effect of [Ala²⁴]MCa on [³H]ryanodine binding is related to experimental *p*Ca conditions. Indeed, no [³H]ryanodine binding stimulation was observed at *p*Ca values ranging between 2 and 7 (Fig. 3*C*).

Characterization of the Effects of MCa and MCa Mutants on Ca²⁺ Release from SR Vesicles—To investigate the effect of

MCa on Ca²⁺ release from heavy SR vesicles, we first actively loaded the vesicles by two consecutive additions of Ca²⁺ (50 μM and 20 μM) in the presence of ATP-Mg²⁺, pyrophosphate, and ATP-regenerating system. After Ca²⁺ loading reaches equilibrium, the addition of 1 μM MCa to the external medium induces Ca²⁺ release as shown in Fig. 4*A*. Similar results were obtained with 100 nM MCa (data not shown), but 1 μM MCa was chosen to allow a comparison with the effects of the lower affinity MCa analogues. External Ca²⁺ level reaches a plateau that corresponds to a new equilibrium between Ca²⁺ release and Ca²⁺ uptake rates as evidenced by the additional change produced by 4 μM A23187 calcium ionophore. The release of Ca²⁺ induced by 1 μM MCa was prevented by preincubating the SR vesicles with 10 μM ruthenium red, demonstrating that MCa-induced calcium release occurs through RyR (Fig. 4*B*). Similarly, the application of 1 μM MCa prevents the release of Ca²⁺ induced by the addition of 500 μM CMC, and conversely, the application of 500 μM CMC prevents an additional release of Ca²⁺ by 1 μM MCa (Fig. 4*C*). These data again demonstrate that MCa re-
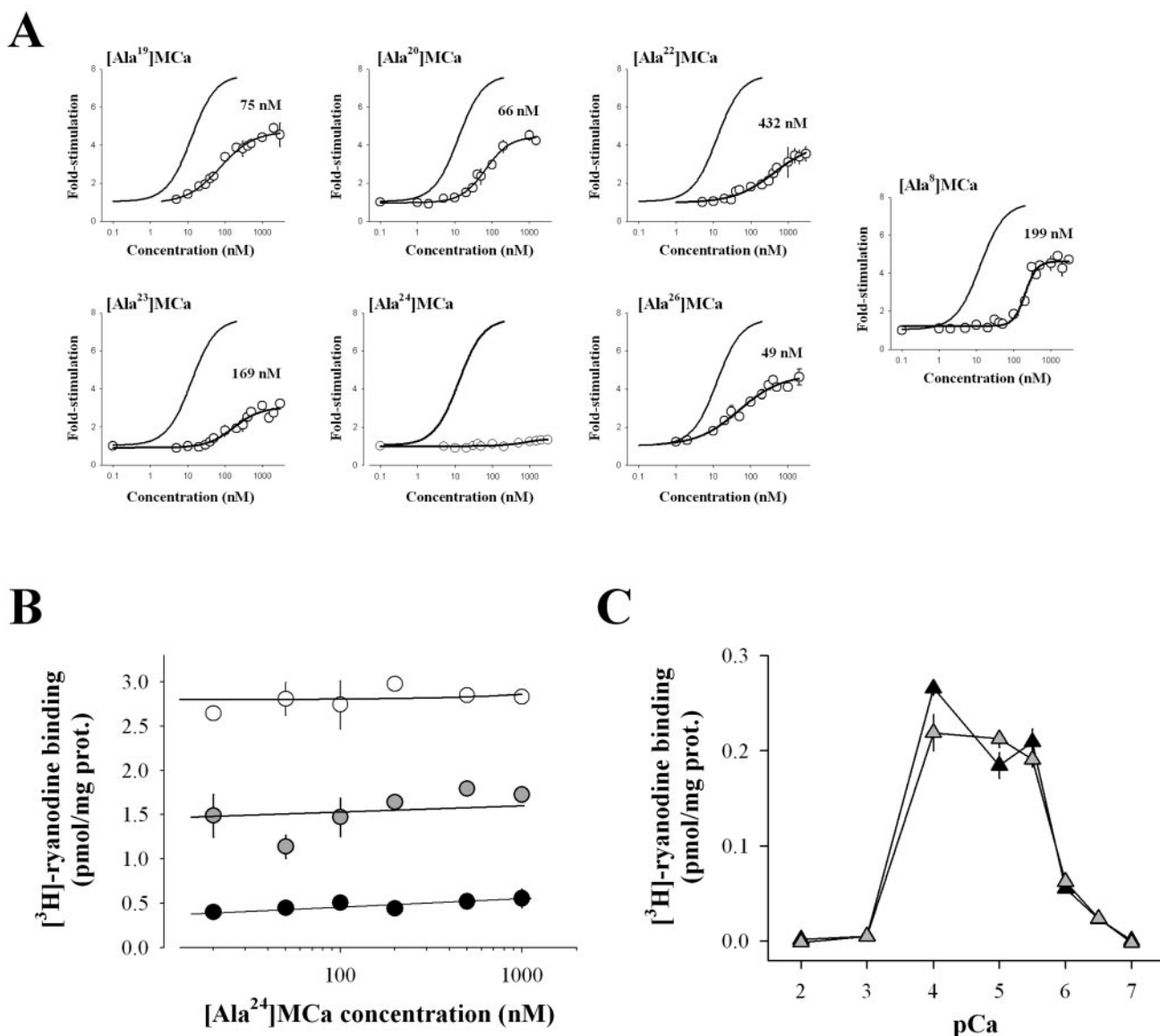
FIG. 3. **Effect of MCa analogues on [³H]ryanodine binding to heavy SR vesicles.** *A*, [³H]ryanodine binding was measured as described in Fig. 2*A* in the presence of various concentrations of each MCa analogue (*open circles*). For comparison, the *solid line* represents the fit of the data shown in Fig. 2*A* for MCa. The EC_{50} values for each analogue were calculated as in Fig. 2*A* and reported in *insert*. *B*, effect of varying [Ala²⁴]MCa concentration on [³H]ryanodine binding measured in the absence (*filled circles*) and presence of 20 (*gray circles*) and 100 nM MCa (*open circles*). *C*, extravesicular Ca^{2+} concentration dependence of [³H]ryanodine binding in the absence (*filled triangles*) and presence of 300 nM [Ala²⁴]MCa (*gray triangles*). The experiments were performed with 5 nM [³H]ryanodine for 2.5 h at 37 °C.

leases Ca^{2+} from SR vesicles by acting on RyR. Fig. 4*D* shows that the application of 1 μM of any one of the mutated MCa analogues induces Ca^{2+} release from SR vesicles with the exception of [Ala²³]MCa and [Ala²⁴]MCa. However, these two last MCa analogues are not equivalent since application of 10 μM [Ala²³]MCa resulted in Ca^{2+} release, whereas 10 μM [Ala²⁴]MCa remained inactive (Fig. 4*E*). The present observation made for [Ala²⁴]MCa is in complete agreement with its lack of effect on [³H]ryanodine binding (Fig. 3*B*). The results obtained with [Ala²³]MCa are also coherent with the data on [³H]ryanodine binding (lower affinity and lower stimulation efficacy), although a discrepancy exists between the [Ala²³]MCa concentration needed for Ca^{2+} release and those inducing an increase in [³H]ryanodine binding.

Modification of RyR1 Calcium Channel Conductance by MCa and Analogues—Application of 200 nM MCa to the *cis* face of the bilayer-recording chamber (cytoplasmic side of RyR1) induces a characteristic long-lasting subconductance state (LLSS) (Fig. 5*A*). This subconductance state represents 60% of

the full conductance state, and the channel spends 54.8 ± 6.2% of its time in this subconductance level. A much less frequent smaller LLSS (48% of the full conductance) was described in earlier reports (5, 6), but the experimental conditions were slightly different (purified RyR1 *versus* junctional SR vesicles and K^+ current *versus* Cs^+ current in previous reports (5, 6)). We next examined whether the LLSS induced by MCa could be correlated to Ca^{2+} release from heavy SR vesicles and stimulation of [³H]ryanodine binding. Therefore, we tested the effect of [Ala²⁴]MCa on the conductance level of RyR1 in lipid bilayers (Fig. 5*B*). Indeed, this mutant peptide has no effect on [³H]ryanodine binding (Fig. 3*A*) nor on the Ca^{2+} release from SR vesicles (Fig. 4*D*). As expected, we show that the application of 200 nM [Ala²⁴]MCa does not induce any LLSS of RyR1. Applications of higher concentrations (up to 750 nM) also were without any effect (data not shown). Conversely, the application of 200 nM of an active MCa analogue, [Ala²⁰]MCa, that conserves MCa-like properties (for [³H]ryanodine binding and Ca^{2+} release from SR vesicles) produces the appearance of the charac-
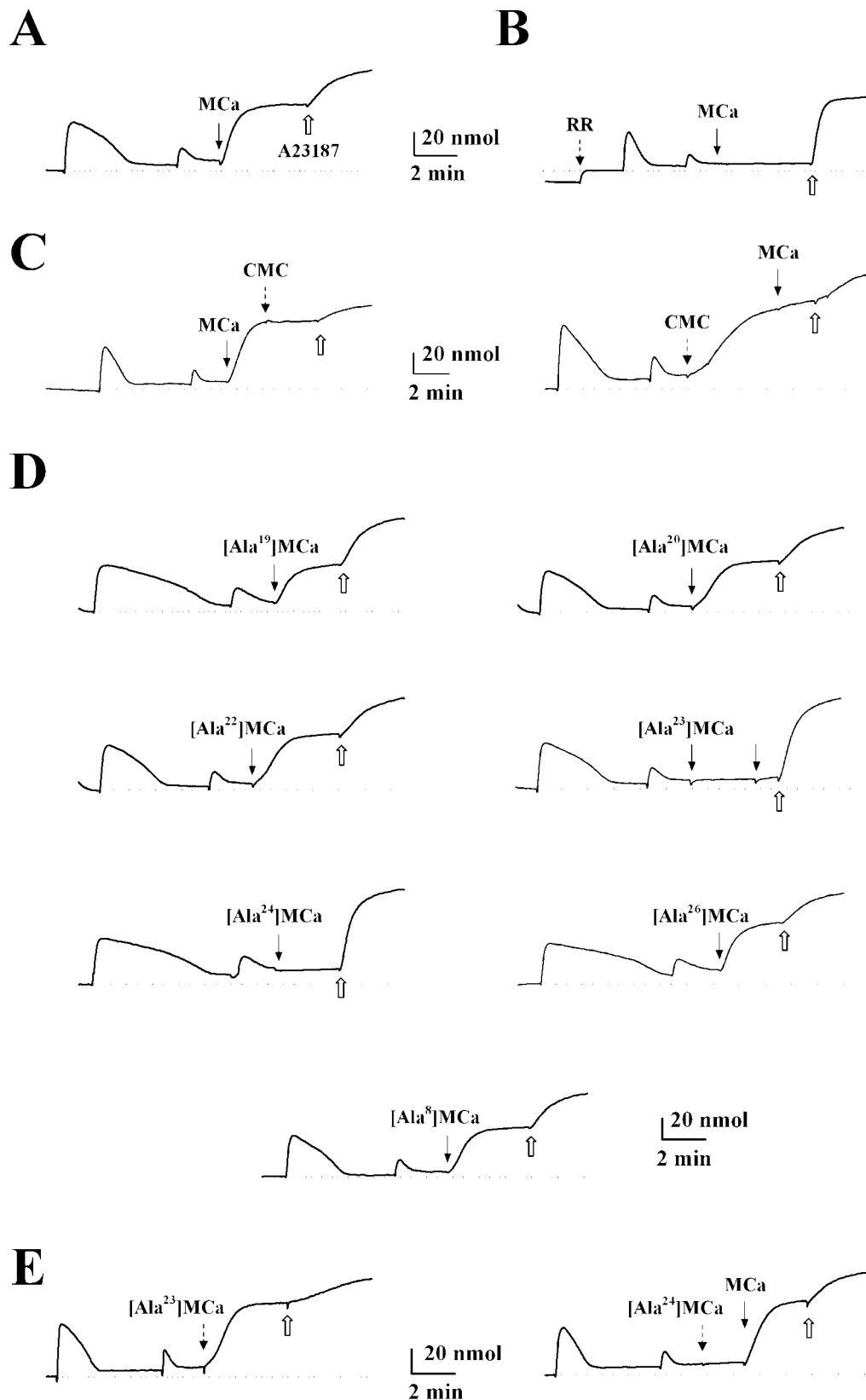
A

MCa A23187

20 nmol
2 min

B

RR MCa

C

CMC
MCa

20 nmol
2 min

MCa
CMC

D

[Ala^{19}]MCa

[Ala^{20}]MCa

[Ala^{22}]MCa

[Ala^{23}]MCa

[Ala^{24}]MCa

[Ala^{26}]MCa

[Ala^{8}]MCa

20 nmol
2 min

E

[Ala^{23}]MCa

MCa
[Ala^{24}]MCa

20 nmol
2 min

FIG. 4. **Ca^{2+} release from heavy SR vesicles induced by MCa and MCa analogues.** *A*, heavy SR vesicles were actively loaded with Ca^{2+} by sequential addition of 50 and 20 μM CaCl$_2$ in the monitoring chamber. After each increment, the absorbance was monitored until the added Ca^{2+} was taken up by SR and the trace relaxed close to its original base line (CaCl$_2$ additions constituting ~70–80% of their loading capacity). In these conditions, the addition of 1 μM MCa produces Ca^{2+} release. The addition of 4 μM A23187 empties the SR vesicles (*open arrow*). Calibration of Ca^{2+} release is performed by two consecutive additions of 20 μM Ca^{2+} (data not shown). *B*, similar experiment as in *A* but with a preliminary application of 10 μM ruthenium red (*RR*). RR produces a deflection of absorbance due to its optical properties. *C*, traces illustrating the lack of effect of 500 μM CMC after MCa application (*left*) and, conversely, the lack of effect of 1 μM MCa after application of 500 μM CMC (*right*). *D*, similar experiments as in *A* but with 1 μM of various MCa analogues. Two consecutive applications were performed for [Ala^{23}]MCa. *E*, traces illustrating the maintenance of effect of MCa on Ca^{2+} release despite the prior application of [Ala^{23}]MCa (*left*) or [Ala^{24}]MCa (*right*).

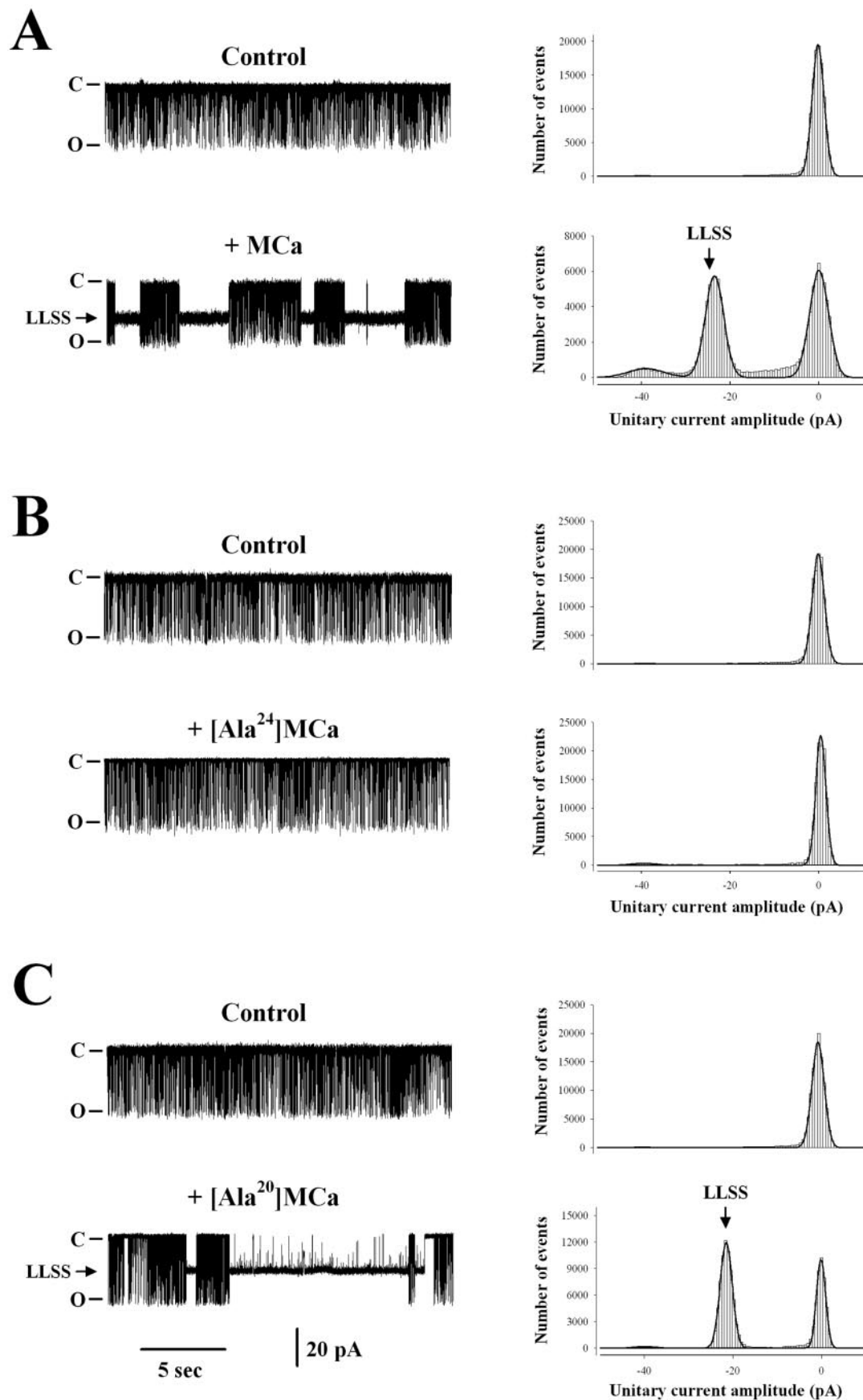*Maurocalcine Efficacy on Skeletal Ryanodine Receptor*

FIG. 5. **MCa but not [Ala²⁴]MCA induces long-lasting openings of RyR1.** Single channel recordings were taken as described under "Experimental Procedures." The holding potential was −80 mV, the conductance of the RyR was approximately 500 pS. The time duration of each record is 20 s. Channel openings are downward deflections, and *C* and *O* designate the closed and opened state of the channel, respectively. Each toxin was applied at a concentration of 200 nM in the *cis* chamber. Free Ca²⁺ concentration was 238 nM in the *cis* chamber. *A*, control and MCa-induced RyR1 channel activity. *Left panel*, representative current traces. *Right panel*, current amplitude histograms. *B*, as in *A* but for [Ala²⁴]MCa. *C*, as in *A* but for [Ala²⁰]MCa.
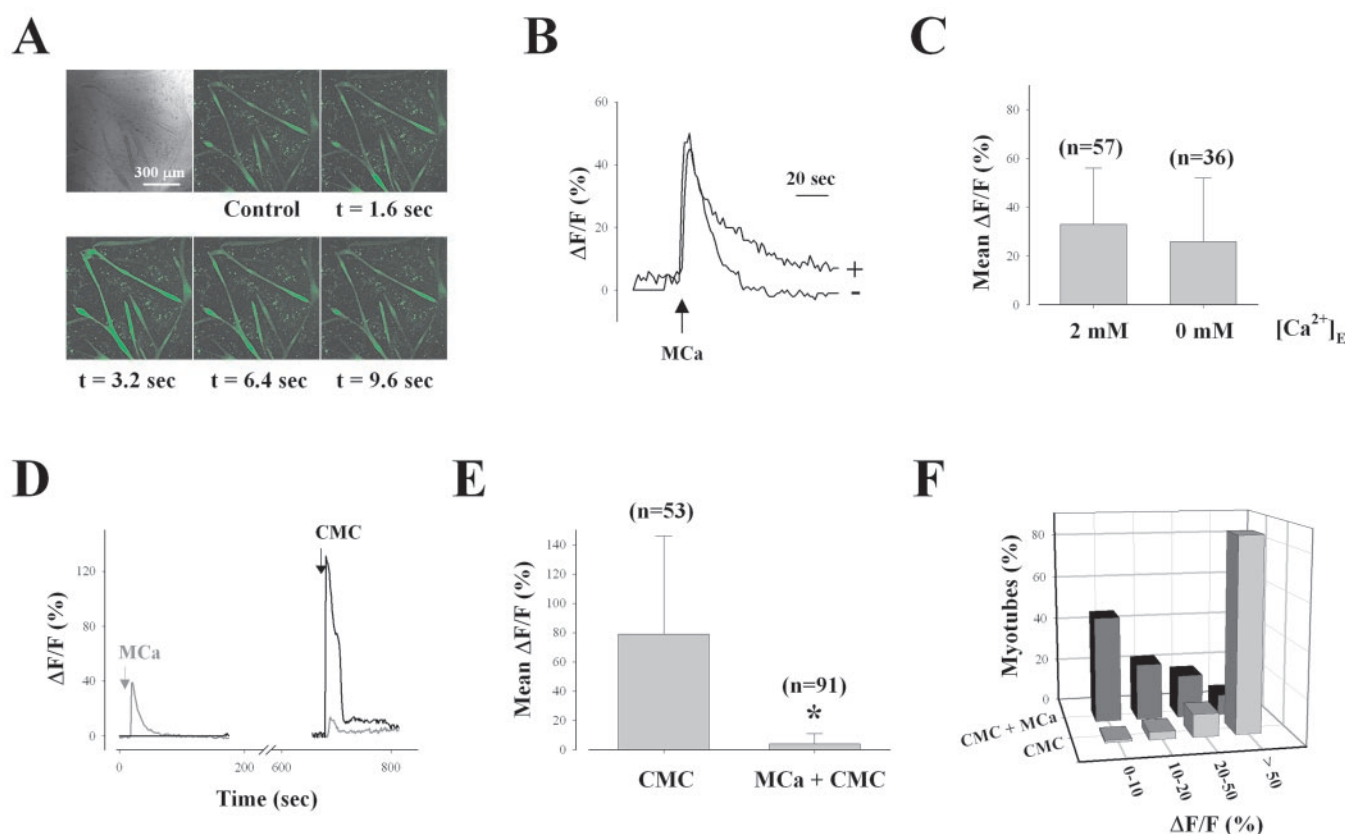
FIG. 6. **MCa induces a cytosolic Ca^{2+} transient in cultured myotubes.** *A*, confocal images of myotubes after 3 days in culture. *Left*, transmitted light image (differential interference contrast). *Right* and *bottom*, Fluo-4 fluorescence images acquired before (*control*) and at indicated times after application of 100 nM MCa. *B*, MCa-induced fluorescence variations of Fluo-4-loaded myotubes measured in the absence (−) and presence (+) of extracellular Ca^{2+}. *C*, mean peak value of Fluo-4 fluorescence variation induced by 100 nM MCa with or without extracellular Ca^{2+}. *D*, fluorescence variation induced by 250 μM CMC without (*black line*) or with (*gray line*) a preapplication of 100 nM MCa. *E*, mean peak value of fluorescence variations induced by CMC without or with preapplication of 100 nM MCa. *F*, percent of myotubes as a function of the peak value of the fluorescence change induced by CMC without or with preapplication of MCa.

teristic LLSS. With this analogue, the LLSS are characterized by a conductance corresponding to 54% of the full-conductance state. Under this condition, the channel spends on average $28 \pm 8.6\%$ of its time in this state (data not shown). The lesser probability for RyR1 to develop in the LLSS in the presence of [Ala[20]]MCa compared with MCa may be related to a lesser ability to stimulate [^{3}H]ryanodine binding (Fig. 3*A*). Other analogues including [Ala[23]]MCa also produced LLSS (data not shown).

Intracellular Ca^{2+} Release in Intact Myotubes Induced by MCa—We next analyzed the effect of MCa on cytosolic Ca^{2+} variations by changes in Fluo-4 fluorescence levels in cultured myotubes. Extracellular application of 100 nM MCa on a group of representative myotubes produces a fast increase in intracellular Ca^{2+} level (Fig. 6*A*). The time course of the change in fluorescence level ($\Delta F/F$) shows that Ca^{2+} increase occurs within 3 s followed by a rapid decrease back to the basal level (Fig. 6*B*). MCa produces a similar elevation in cytosolic Ca^{2+} when extracellular medium is supplemented with 50 μM La^{3+} and deprived of Ca^{2+} by the addition of 1 mM EGTA (Fig. 6*B*). This observation demonstrates that MCa-induced Ca^{2+} mobilization occurs from internal sources. An analysis of the average change in fluorescence level confirms that there is no significant difference in cytosolic Ca^{2+} elevation in the absence or presence of extracellular Ca^{2+} (Fig. 6*C*). In similar experimental conditions, external application of 250 μM CMC also induces a rapid and transient Ca^{2+} elevation (Fig. 6*D*) (24). A prior incubation of the myotube with 100 nM MCa almost totally prevents CMC-induced peak Ca^{2+} elevation (Fig. 6*D*). This observation was confirmed by an average quantification of

fluorescence variation (mean $\Delta F/F = 79 \pm 67$ ($n = 53$) for CMC alone *versus* 4 ± 7 ($n = 91$) for CMC after MCa) (Fig. 6*E*). We also analyzed the cell variability in response to CMC alone or CMC after MCa application (Fig. 6*F*). In the presence of CMC, most myotubes (85.6%) produce important changes in fluorescence ($\Delta F/F > 50\%$), whereas after incubation with MCa, an opposite profile of responses is observed with 47% of the cells showing <10% change in fluorescence ($\Delta F/F = 0–10\%$). These results demonstrate that the CMC-sensitive Ca^{2+} stores are also MCa-sensitive. Because CMC is known to act on intracellular Ca^{2+} stores by the bias of RyR (2), this is another indication that MCa acts on RyR-dependent Ca^{2+} stores. To confirm that the effect of MCa on Ca^{2+} elevation is the result of an interaction with RyR, we also tested the effect of the mutant [Ala[24]]MCa. We show that it is unable (i) to produce a Ca^{2+} release from myotubes (Fig. 7*A*) and (ii) to modify CMC effect (Fig. 7*B*).

DISCUSSION

In skeletal muscles, RyR1 appears to represent the main target of MCa. We have previously shown that this toxin stimulates [^{3}H]ryanodine binding, stabilizes RyR1 into a subconductance state, and produces Ca^{2+} release from heavy SR vesicles. In this work, we further investigated the biochemical and functional properties of MCa. Using synthetic mutated analogues of MCa, we defined some critical amino acid residues of MCa that are required for its effects on RyR1. We also show for the first time that MCa is able to induce intracellular Ca^{2+} release in intact myotubes. This effect is conserved in the absence of external Ca^{2+}, demonstrating that the increase in
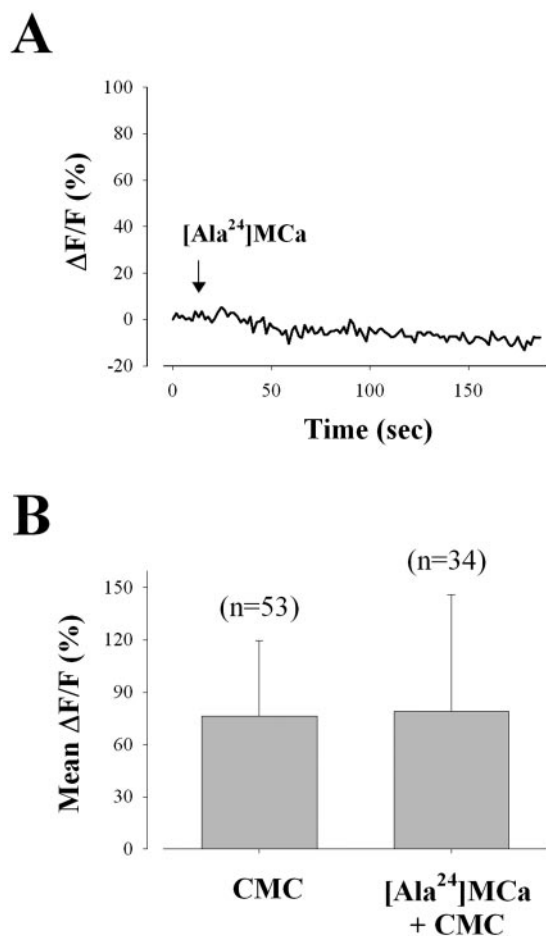
FIG. 7. **[Ala²⁴]MCa does not induce Ca²⁺ release in intact myotubes.** *A*, variation of the cytoplasmic Ca^{2+} concentration upon external application of 1 μM [Ala²⁴]MCa was measured as described in Fig. 6. *B*, mean peak value of fluorescence variations induced by 250 μM CMC without or with preapplication of 1 μM [Ala²⁴]MCa.

cytoplasmic Ca^{2+} concentration is due to the release of Ca^{2+} from internal stores. In these conditions, Ca^{2+} release induced by CMC, a RyR1 agonist, is completely inhibited by the preapplication of MCa. Conversely, the application of the inactive [Ala²⁴]MCa analogue does not induce any Ca^{2+} release from internal stores nor does it inhibit CMC-induced Ca^{2+} release. These data demonstrate that Ca^{2+} release induced by MCa occurs through RyR1 activation. The cellular effect of MCa is of the greatest importance because it demonstrates that the toxic effect of the toxin can be explained by its action on RyR1 despite the intracellular location of this target. This result also reveals that MCa has the ability to cross the plasma membrane of skeletal muscle cells, a property that is shared by some other basic peptides (25). Cell penetration is expected to occur rapidly as Ca^{2+} elevation can be observed a few seconds after external application of MCa.

We have identified Arg²⁴ as a crucial amino acid residue for the effects of MCa. Indeed, the replacement of Arg²⁴ by an alanine induces a complete loss of MCa effects on [³H]ryanodine binding, on the appearance of subconductance events, on Ca^{2+} release from SR vesicles, and on intact myotubes. Conversely, mutated analogues that appeared less crucial for RyR1 recognition all kept similar profiles of effects than did MCa. Our data demonstrate that the loss of effects of [Ala²⁴]MCa is because of the inability of this analogue to bind onto RyR1. Indeed, we show the absence of [Ala²⁴]MCa effect on MCa-induced stimulation of [³H]ryanodine binding and on MCa-induced Ca^{2+} release from SR vesicles. MCa and other func-

tional analogues, such as [Ala²⁰]MCa, have in common the ability to induce long-lived subconductance states of RyR1. The appearance of this subconductance state probably explains the release of Ca^{2+} from SR vesicles and in part the stimulation of [³H]ryanodine binding. This finding is coherent with the hypothesis that ryanodine preferentially binds onto the open state of RyR1 (26). There are interesting functional similarities between ryanodine and MCa. Both appear able to induce subconductance states, and MCa favors [³H]ryanodine binding. These data strongly suggest the existence of a positive synergy between the binding sites of the two molecules on RyR1. This synergy is further evidenced by the fact that MCa increases by a factor of 6.1-fold the affinity of [³H]ryanodine for RyR1. In addition, in the presence of MCa, we observed a shift to lower Ca^{2+} concentrations of the Ca^{2+} stimulatory effect on [³H]ryanodine binding and a shift to higher Ca^{2+} concentrations of the Ca^{2+} inhibitory effect on [³H]ryanodine binding. These data are in favor of a model in which the binding of either one of these two molecules, ryanodine or MCa, produces a chain of conformational events, leading to the appearance of subconductance states. All of the active MCa analogues that we tested stimulated [³H]ryanodine binding with higher EC_{50} values than MCa itself. We also measured a reduced ability to stimulate [³H]ryanodine binding. Although the substituted amino acid residues of MCa do not appear decisive for the interaction with RyR1, they seem to contribute to some extent to the binding site recognition. In addition, they also appear to participate to the conformational events that lead to the modification of the low affinity ryanodine binding sites. We would expect that more drastic substitutions within MCa lead to modifications in the level of RyR1 subconductance states and/or in the time spent in these subconductance states. Indeed, it has been observed that IpTxA, which shares 82% sequence identity with MCa, induces a subconductance state of RyR significantly different from the one triggered by MCa (25% of the full-conductance state for IpTxA *versus* 58% for MCa) (9, 10). Moreover, in contrast to what is observed with IpTxA, LLSS induced by MCa and its analogues are polarity-independent. Similarly, the domain A of the α_1 subunit of DHPR that shares sequence similarities with both MCa and IpTxA also induces a subconductance state different from those observed with the toxin (65 and 86% of the full-conductance state for domain A) (6). Based on sequence identity, it is probable that MCa and IpTxA bind more than one common site(s) or regions on the RyR1 tetramer. Interestingly, the binding of two structurally related molecules on the same channel can produce highly different conductance states of RyR1. Therefore, it is tempting to postulate that once MCa or IpTxA is bound on RyR1, structural modification of these ligands could produce important changes in the conductance properties of RyR1. This concept of RyR1 conductance modulation could be applied to domain A to provide an explanation for its role in the regulation of RyR1 function. Recently, it was proposed that the three-dimensional structural surface of MCa and IpTxA mimics that of domain A (23). It would be interesting to investigate whether conformational changes in domain A during membrane depolarization are of nature to modify RyR1 channel conductance.

REFERENCES

1. Mackrill, J. J. (1999) *Biochem. J.* **337,** 345–361
2. Zorzato, F., Scutari, E., Tegazzin, V., Clementi, E., and Treves, S. (1993) *Mol. Pharmacol.* **44,** 1192–1201
3. Jona, I., Szegedi, C., Sarkozi, S., Szentesi, P., Csernoch, L., and Kovacs, L. (2001) *Pflügers Arch. Eur. J. Physiol.* **441,** 729–738
4. Valdivia, H. H., Kirby, M. S., Lederer, W. J., and Coronado, R. (1992) *Proc. Natl. Acad. Sci. U. S. A.* **99,** 12185–12189
5. Fajloun, Z., Kharrat, R., Chen, L., Lecomte, C., di Luccio, E., Bichet, D., El Ayeb, M., Rochat, H., Allen, P. D., Pessah, I. N., De Waard, M., and Sabatier, J. M. (2000) *FEBS Lett.* **469,** 179–185
6. Chen, L., Estève, E., Sabatier, J. M., Ronjat, M., De Waard, M., Allen, P. D.,

and Pessah, I. N. (2003) *J. Biol. Chem.* **278,** 16095–16106

7. El Hayek, R., Lokuta, A. J., Arévalo, C., and Valdivia, H. H. (1995) *J. Biol. Chem.* **270,** 28696–28704

8. Zamudio, F. Z., Gurrola, G. B., Arévalo, C., Sreekumar, R., Walker, J. W., Valdivia, H. H., and Possani, L. B. (1997) *FEBS Lett.* **405,** 385–389

9. Gurrola, G. B., Arévalo, C., Sreekumar, R., Lokuta, A. J., Walker, J. W., and Valdivia, H. H. (1999) *J. Biol. Chem.* **274,** 7879–7886

10. Simeoni, I., Rossi, D., Zhu, X., Garcia, J., Valdivia, H. H., and Sorrentino, V. (2001) *FEBS Lett.* **508,** 5–10

11. El Hayek, R., and Ikemoto, N. (1998) *Biochemistry* **37,** 7015–7020

12. Proenza, C., Wilkens, C. M., and Beam, K. G. (2000) *J. Biol. Chem.* **275,** 29235–29237

13. Ahern, C. A., Bhattacharya, D., Mortenson, L., and Coronado, R. (2001) *Biophys. J.* **81,** 3294–3307

14. O'Reilly, F. N., Robert, M., Jona, I., Szegedi, C., Albrieux, M., Geib, S., De Waard, M., Villaz, M., and Ronjat, M. (2002) *Biophys. J.* **82,** 145–155

15. Merrifield, R. B. (1986) *Science* **232,** 341–347

16. Kim, D. H., Onhishi, S. T., and Ikemoto, N. (1983) *J. Biol. Chem.* **258,** 9662–9668

17. Marty, I., Thevenon, D., Scotto, C., Groh, S., Sainnier, S., Robert, M., Grunwald, D., and Villaz, M. (2000) *J. Biol. Chem.* **275,** 8206–8212

18. Palade, P. (1987) *J. Biol. Chem.* **262,** 6142–6148

19. Lai, F A., Erickson, H. P., Rousseau, E., Liu, Q. Y., and Meissner, G. (1988) *Nature* **331,** 315–319

20. Herrmann-Frank, A., Reacher, M., Sarkozi, S., Mohr, U., and Lehmann-Horn, F. (1996) *Biochim. Biophys. Acta* **1289,** 31–40

21. Fabiato, A. (1988) *Methods Enzymol.* **157,** 378–417

22. Mosbah, A., Kharrat, R., Fajloun, Z., Renisio, J. G., Blanc, E., Sabatier, J. M., El Ayeb, M., and Darbon, H. (2000) *Proteins* **40,** 436–442

23. Green, D., Pace, S., Curtis, S. M., Sakowska, M., Lamb, G. D., Dulhunty, A. F., and Casarotto, M. G. (2003) *Biochem. J.* **370,** 517–527

24. Gschwend, M. H., Rüdel, R., Brinkmeier, H., Taylor, S. R., and Föhr, K. J. (1999) *Eur. J. Physiol.* **438,** 101–106

25. Lindgren, M., Hällbrink, M., Proschiantz, A., and Langer, Ü. (2000) *Trends Physiol. Sci.* **21,** 99–103

26. Coronado, R., Morrissette, J., Sukhareva, M., and Vaugham, D. M. (1994) *Am. J. Physiol.* **266,** C1485–C1504